



Investigation of Submarine Groundwater Discharge using Thermal Satellite and Radon mapping along the East Coast of the Tamil Nadu and Pondicherry Region, India

A. Rajesh Kanna ^a, K. Srinivasamoorthy ^{a,*}, G. Ponnumani ^a, C. Babu ^a, R. Prakash ^a,
S. Gopinath ^a

^a Department of Earth Sciences, School of Physical, Chemical and Applied Sciences, Pondicherry University, Puducherry-605014, India.

* Corresponding Author: moorthy_ks@yahoo.com

Received: 21-02-2021, Revised: 09-05-2021, Accepted: 11-05-2021, Published: 23-05-2021

Abstract: Submarine groundwater discharge (SGD) demarcated as a significant component of hydrological cycle found to discharge greater volumes of terrestrial fresh and recirculated seawater to the ocean associated with chemical constituents (nutrients, metals, and organic compounds) aided by downward hydraulic gradient and sediment-water exchange. Delineating SGD is of primal significance due to the transport of nutrients and contaminants due to domestic, industrial, and agricultural practices that influence the coastal water quality, ecosystems, and geochemical cycles. An attempt has been made to demarcate the SGD using thermal infrared images and radon-222 (²²²Rn) isotope. Thermal infrared images processed from LANDSAT-8 data suggest prominent freshwater fluxes with higher temperature anomalies noted in Cuddalore and Nagapattinam districts, and lower temperature noted along northern and southern parts of the study area suggest saline/recirculated discharge. Groundwater samples were collected along the coastal regions to analyze Radon and Physico-chemical constituents. Radon in groundwater ranges between 127.39 Bq m⁻³ and 2643.41 Bq m⁻³ with an average of 767.80 Bq m⁻³. Calculated SGD fluxes range between -1.0 to 26.5 with an average of 10.32 m day⁻¹. Comparison of the thermal infrared image with physio-chemical parameters and Radon suggest fresh, terrestrial SGD fluxes confined to the central parts of the study area and lower fluxes observed along with the northern and southern parts of the study area advocate impact due to seawater intrusion and recirculated seawater influence.

Keywords: SGD, Thermal infrared image, SST, Radon fluxes, Recirculated seawater, East coast of South India.

1. Introduction

Submarine groundwater discharge (SGD) demarcated as a discharge of terrestrial (fresh) groundwater influenced by hydraulic gradient from land aquifers to the ocean and recirculated seawater through the aquifer sediments influenced by currents, waves, and tides [1]. SGD to the nearshore competes for river water inputs [2] both in volume and dissolved chemical constituents [2,3]. Due to greater concentrations of dissolved chemical constituents, including nutrients, SGD is isolated as a significant pathway to alter biogeochemistry and coastal ecosystems [4-6]. Factors like superfluous growth of marine phytoplankton and algae found to influence the marine habitats, species and ecosystem due to nutrient discharge via SGD resulting in eutrophication and oxygen depletion termed as hypoxia [7-10]. In localities of aquifer uncleanness due to sewage and industrial activities might also stimulate coastal contamination [11,12]. The impact of the human population influencing coastal aquifers is found to induce groundwater aided by increased supply of chemical constituents (major ions, trace elements) and nutrients resulting in alteration of coastal ecosystems [13].

Hence recognition of SGD is of greater importance to isolate pathways of nutrients, trace elements, and other contaminants in order to develop tools and pathways to assess regional impacts. Due to varying spatial and temporal patterns of SGD, it is challenging to evaluate discharges over a greater aerial extent [14,4]. By considering the need, an attempt has been made in the proposed study to evaluate the use of aerial thermal infrared (TIR) imagery using LANDSAT-8 data sets, along with chemical concentrations like salinity and Radon to quantify SGD fluxes to the Bay of Bengal.

Thermal infrared (TIR) images can resolve the spatial variation of groundwater discharge due to contrasting temperature and density varying waters (saline and fresh) [15,16]. Fresh groundwater tends to exist at average annual groundwater temperature compared with ambient saline surface-waters [17,18]. Hence temperature of fresh groundwater will be either greater or lesser compared with saline waters and found to be influenced by seasonal variations [19] where SGD will be more relaxed than surface water in summer months and through the monsoon, warmer SGD is expected than the surface water [20].

Naturally occurring isotopes produced from uranium and thorium decay series have been used to demarcate groundwater discharge sites isolated using TIR imageries. Radon (^{222}Rn) is used as a proxy to identify areas of significant groundwater discharge due to higher magnitude in groundwater compared to seawater, its conservative nature, shorter half-life, and ease in measurement [21]. Radon (^{222}Rn) is a non-reactive noble gas with a half-life of 3.82 days generated due to sediment recoil from uranium and thorium disintegration present in the aquifer sediments [22,23]. For the present study, TIR and Radon have been used to isolate groundwater discharge sites to the Bay of Bengal.

2. Study Area

The study area falls amid the Cauvery delta regime between Gadilam and Agniar rivers that encompasses Tamilnadu and Pondicherry coastal regions of South India between latitude $10^{\circ}20'0''$ N and $11^{\circ}50'0''$ N and longitude $79^{\circ}20'0''$ E and $79^{\circ}50'00''$ E with a full coastal stretch of about 200 km (Fig. 1). The climate of the study area is influenced by adjoining Bay of Bengal experiencing hot and humid climatic conditions with temperature varying between 19.3° C to 40.6° C with sharp fall in night temperatures during the monsoon period with a mean annual temperature of about 31° C. The summer season is from March to May, noted with maximum temperature, and during December to February, the minimum temperature is observed (CGWB 2008) [24]. The relative humidity ranges between 62 % and 85 % throughout the year with higher (85 %) observed during November and lower (62%) noted during the month of February and remains low until May. Evaporation is higher (10.8 mm) from May to August and lowers during November (2.7 mm). Winds are primarily north-westerly or westerly during May and September, and from October to February, winds are northeasterly or northerly. Wind speed is higher during May (12.5 Km/hr) and lowest in October (7.4 km/hr).

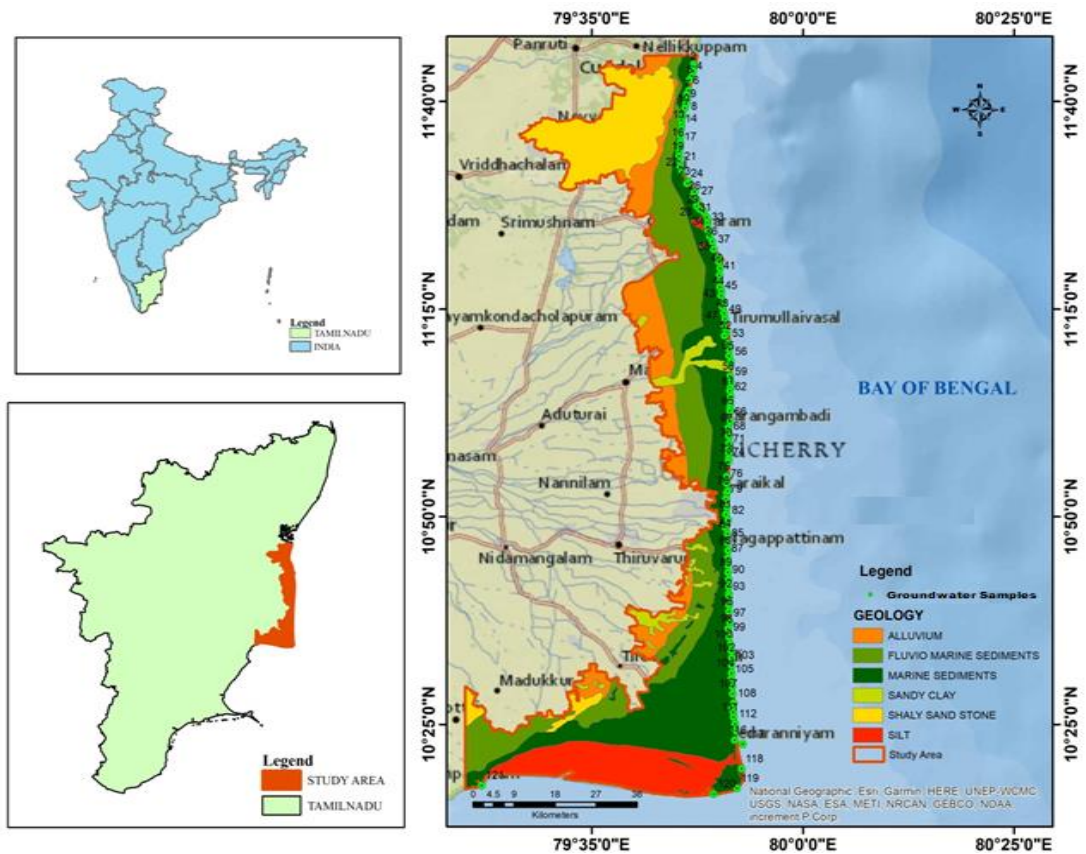


Figure 1. Study area location, geology, and groundwater sample locations

The average annual rainfall over the study area varies from about 1050 mm to about 1400 mm (CGWB 2009) [25]. Rainfall of the study area is influenced by northeast and southwest monsoons. During the northeast monsoon (October to December) about 52% of the rainfall happens and about 41% during the southwest monsoon (June to September). The rest of the precipitation happens during the summer (March to May) and winter (January and February) seasons, respectively (CGWB 2015) [26].

The study area's geology is covered by recent deposits of marine and fluvial marine sediments and small patches of alluvium, sandy clay, silt, and cretaceous deposit of shaly sandstone. The study area is part of the composite east-flowing river basin having Cauvery and Vennar sub-basins and drained by Gadilam, Pennaiyar, Vellar, Kollidam, Cauvery, Virasolanar, Uppanar, Arasalar, Tirumalairajan Aru, Vetter, Kedurai Aru, Pandavai Aru, Vedaranyam canal, and Harichandra Nadi (CGWB 2008 and CGWB 2009). The present geomorphological setup of the study area is due to the action of significant rivers and their distributaries, oscillations in the sea level, tidal effect of the Bay of Bengal, and wind velocities.

3. Materials and methods

The present study demarcates SGD hot spots using sea surface temperature (SST), water index, and Radon (^{222}Rn) based assessment. SST of the present study area has been calculated by processing the thermal infrared image (TIR) of LANDSAT - 8 data. LANDSAT - 8 satellite data set from USGS Earth Explorer website has been used. For the present study TIR bands, 10 and 11 were utilized to estimate temperature differences in sea surface, and bands 4 and 5 were utilized for Normalized Differential Vegetation Index (NDVI) generation.

Table 1. Bands, wavelength, and resolution for the present study

Bands	Wavelength (micrometers)	Resolution (meters)
Band 1 -Ultra blue, (coastal/aerosol)	0.43-0.45	30
Band 2 Blue	0.45-0.51	30
Band 3 Green	0.53-0.59	30
Band 4 Red	0.64-0.67	30
Band 5 Near Infra-Red	0.85-0.88	30
Band 6 Short Infrared (SWIR)1	1.57-1.65	30
Band 7 Short wave infrared (SWIR)2	2.11-2.29	30
Band 8 Panchromatic	0.50-0.68	15
Band 9 Cirrus	1.36-1.38	30
Band 10 Thermal Infrared (TIRS)1	10.6-11.19	100
Band 11 Thermal Infrared (TIRS)2	11.50-12.51	100

Satellite data products over the Tamil Nadu coast of January 2019 were used for the present study. Landsat 8 gives metadata information for thermal constant, rescaling factor value

which has been utilized for the calculation of the Land Surface Temperature. The wavelength and resolution of Landsat 8 utilized for the present study are given in Table-1.

One hundred seventeen groundwater samples were collected during low tide at a transect parallel to the East coast of Tamilnadu (Fig. 1) and analyzed within 3 to 6 hours after sampling for minimum loss of radon gas. Radon (^{222}Rn) was determined using the radon emanometry method, designed by Polltech Instruments Pvt. Ltd., Mumbai, India. Radon activity in the water samples has been calculated using an equation suggested by [27].

$$222\text{Rn} (Bq L^{-1}) = \frac{6.97 \times 10^{-2} \times D}{V \times E \times (1 - e^{-\lambda t}) \times e^{-\lambda T}} \quad (1.1)$$

Where D represents above background counts, λ being radon decay constant as ($2.098 \times 10^{-6} \text{ s}^{-1}$), E is the scintillation cell efficiency (74%), V being the water volume, T being the delay in radon counting after groundwater sampling (s), and t being the counting duration(s). Physicochemical parameters like EC, pH, TDS, salinity, and DO have been analyzed in the field using the Hanna water analyzer.

4. Result and Discussion

4.1. The process attempted to retrieve Sea Surface Temperature

Landsat 8 satellite data product for Tamilnadu coast representing January 2019 downloaded from USGS website has been used to acquire the sea surface temperature for the study area (Fig. 2). The data product used was acquired during day time, with path/row 142/52 and 142/53 with cloud cover <15 % acquired on 10th January 2019 at 04:59 a.m. All the data sets were resampled attempting nearest neighbor method, projected to Universal Transverse Mercator (UTM) coordinate system with WGS84 datum and zone 44. The steps discussed below were attempted to identify thermal anomalies.

4.1.1. Top of Atmosphere (TOA) spectral radiance

Using rescaled radiance factor, the infra-red pixel digital numbers (DN values) of Landsat TIR band ten were converted to TOA spectral radiance adopting formulae as noted below [28,29]:

$$L_{\lambda \text{ TOA}} = M_L \times Q_{\text{cal}} + A_L \quad (2.1)$$

Where, $L_{\lambda \text{ TOA}}$ recommends spectral radiance expressed in Watts ($\text{m}^2 \cdot \text{sr} \cdot \mu\text{m}^{-1}$), M_L suggests rescaling factor for band 10, A_L proposes the rescaling factor (0.1) for band ten, and Q_{cal} represents the quantized and calibrated standard product pixel values (DN).

4.1.2. Top of Atmosphere (TOA) Brightness Temperature

The spectral radiance values are converted to temperature using the constant thermal values from the satellite metadata file adopting the formula.

$$BT = \frac{K_2}{\ln\left(\frac{K_1}{L_\lambda} + 1\right)} - 273.15 \quad (2.2)$$

BT represents the TOA brightness temperature represented in °C, L_λ being the spectral radiance, K_1 and K_2 are the band's precise thermal conversion metadata files acquired from satellite data files. In order to calculate the temperature in °C, absolute zero is added that approximates -273.15. Due to lower water vapor in the atmosphere, atmospheric values are not considered for calculating SST.

4.1.3. Normalized Differential Vegetation Index (NDVI)

The Normalized Differential Vegetation Index (NDVI) that isolates varying land cover types is a standardized vegetation index calculated using Near Infra-red (Band 5) and Red (Band 4) bands using the equation suggested below.

$$NDVI = \frac{NIR-RED}{NIR+RED} \quad (2.3)$$

RED is DN values from the RED band, and NIR is DN values from the Near-Infrared band. The further calculation is required to assess land surface emissivity and sea surface temperature.

4.1.4. Land Surface Emissivity (LSE)

Land surface emissivity (LSE) is calculated from the NDVI values that suggest the average emissivity values from individual elements on the earth's surface attempted using the equation suggested below.

$$PV = \left[\frac{NDVI-NDVI_{min}}{NDVI_{max}+NDVI_{min}} \right]^2 \quad (2.4)$$

Where PV being the vegetation proportionality, NDVI being the DN values gathered from NDVI Image, NDVI min is the minimum DN values adopted from NDVI Image, and NDVI max being the maximum DN values gathered from NDVI image calculated using the formula:

$$E = 0.0004xPV + 0.986 \quad (2.5)$$

Where E is the land surface emissivity, and PV is the vegetation proportionality.

4.1.5. Sea Surface Temperature (SST)

The Sea Surface Temperature (SST) is the sea surface temperature calculated using Top of atmosphere brightness temperature, Wavelength of emitted radiance, and Land Surface Emissivity adopting the equation suggested below.

$$SST = \left(\frac{BT}{1}\right) + W_x \left(\frac{BT}{14380}\right) x \ln(E) \quad (2.6)$$

4.2. Quantification of SGD fluxes

A total of 302 water samples were collected during low tide at a transect parallel to the coast (Figure.1), and the height of the tide ranges between 0.1m and 0.73 m during the study. The statistical results of ^{222}Rn and physicochemical parameters for groundwater samples are given in the table. 2. Radon in groundwater ranges between 127.39 to 2643.41 Bq/m^3 with an average of 767.80 Bq/m^3 . Greater radon activity in groundwater samples suggests fresh groundwater discharge and declining values suggest influence due to recirculated seawater [32]. The salinity of groundwater samples ranges between 0.22 to 10.20 ppt with an average of 2.44 ppt. Salinity and radon values were found to correlate where excess salinity correlated with lower Radon and lower salinity correlated with greater Radon suggesting the influence of fresh and recirculated seawater [33, 34]. Electrical conductivity (EC) of coastal groundwater ranges between 45,800.00 to 380.00 $\mu\text{S cm}^{-1}$ with an average of 506.00 $\mu\text{S cm}^{-1}$ signifying well-mixed groundwater with the influence of tides along with alluvium formation noted with more excellent permeability and well-sorted sand patterns and rainfall during northeast monsoons might have influenced electrical conductivity values [35]. The suitability of water for various purposes can be aided by the variation in Total Dissolved Solids (TDS). TDS ranges between 221.00 to 26500.00 mg L^{-1} with an average of 2933.26 mg L^{-1} suggesting the influence of fresh groundwater mixing with sea and vice versa in specific locations suggesting influence due to tides. The statistics of the data sets are represented in (Figure. 3). The temperature of water ranges between 24.80 to 29.80°C; variation in groundwater temperature might be due to the spatial and temporal variation of groundwater and seawater temperature [20].

Table 2. Statistics of ^{222}Rn and Physio-Chemical parameters attempted in the study area

	Radon	Salinity	Electrical Conductivity (EC)	Total Dissolved Solid (TDS)	Temperature
Max	2643.41	10.20	45.80	26500.00	29.80
Min	127.39	0.22	0.38	221.00	24.00
Avg	767.80	2.44	5.06	2933.26	27.83

(Radon expressed as Bq/m^3 , salinity as ppt, Electrical Conductivity as $\mu\text{S/cm}$, Total Dissolved solids as mg L^{-1} and temperature in °C).

(Radon expressed as Bq/m^3 , salinity as ppt, Electrical Conductivity as $\mu\text{S/cm}$, Total Dissolved solids as mgL^{-1} and temperature in °C). The SGD flux estimated by Radon based conceptual model as suggested by [36]. In order to isolate Radon influenced SGD fluxes, Radon in groundwater should be balanced for various sources and sinks that include: excess Radon due to water dissolved radium (^{226}Ra), tidal variations, loss to the atmosphere, diffusive flux from sediments, mixing of radon low offshore water, tidal dynamics, atmospheric losses, sediment diffusivity and mixing loss due to lower radon water offshore. The above-discussed sources and sinks influence the radon balance for a given time [37]. The statistical data for ^{222}Rn and physical parameters have been given in the table. 2.

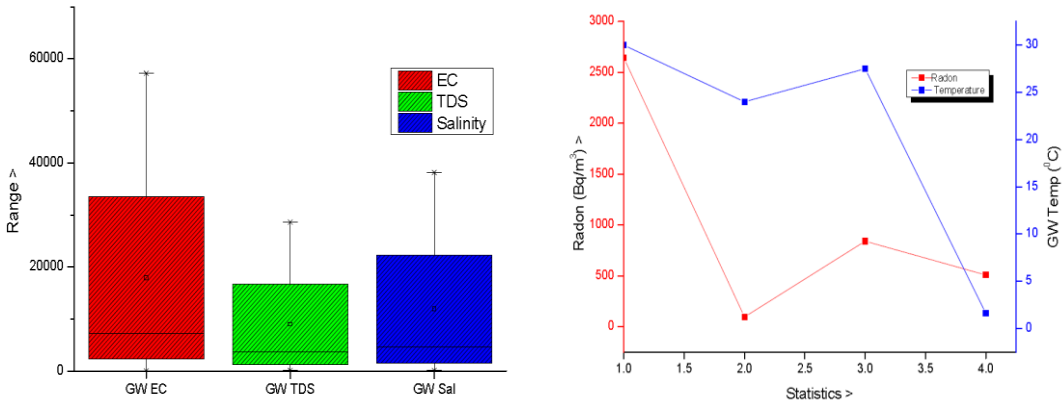


Figure 3. Statistical comparison of physical parameters

The measured ²²²Rn is corrected to isolate the Radon attributed SGD fluxes by dividing the ²²²Rn estimated fluxes by groundwater measured ²²²Rn concentrations for a given study area. The Radon derived SGD flux is calculated using the equation given below [32].

$$FSGD = F_t + F_{sed} + F_i + F_{atm} + F_o + F_{mix} \quad (3.1)$$

Here, FSGD proposes the measured SGD due to Radon, F_t suggests radon variance during consecutive sampling hours, F_{sed} being the Radon that escapes from aquifer sediments, F_o being the Radon that voyage due to low tide, F_{atm} being the radon discharge to atmosphere, F_i proposes radon movement during high tide, and F_{mix} suggests the mixing loss of Radon.

The SGD fluxes are generally calculated by considering the Radon attributed fluxes (FSGD) attempted by dividing the groundwater measured radon end member. The SGD flux calculation is attempted from the equation suggested below:

$$QSGD = FSGD / 222_{Rn_{gw}} \quad (3.2)$$

Here, QSGD is the terrestrial, fresh SGD flux usually measured as m/d, FSGD being the ascribed ²²²Rn flux measured in Bq/m²h¹, and ²²²Rn gw is the groundwater attributed Radon usually measured as Bq/m³.

4.2.1. Atmospheric loss

Radon in groundwater is calculated by considering the air radon with partition coefficient as suggested below:

$$\alpha = 0.105 + 0.405e^{-0.0502T} \quad (3.3)$$

Here, α implies partition coefficient, and T point toward water temperature measured in °C

The significant loss of Radon is mainly by diffusion to the atmosphere. The estimation is attempted utilizing the molecular diffusion due to ^{222}Rn gradients and wind transfer influenced due to wind velocity and temperature variance. Radon gas is partially soluble in water and mixing aided across the air-water interface and found in imbalanced phases. At equilibrium:

$$C_w = \alpha C_a \quad (3.4)$$

Here, C_w indicates measured Radon in water (Bqm^{-3}), C_a being the ^{222}Rn presence in the atmosphere (Bq m^{-3}) and α suggests the partition coefficient. Once $C_w > \alpha C_a$, diffuse of ^{222}Rn will be noted from water phase to atmosphere, and the loss is calculated adopting equation suggested by Eckerman et al. 2012 [38] as:

$$F_{atm} = k(C_w - \alpha C_a) \quad (3.5)$$

Hence, F_{atm} suggests the Radon diffusive across the air-water interface ($\text{Bq m}^{-2} \text{h}^{-1}$); k being the velocity of gas transfer (m s^{-1}). The relationship between wind speed and velocity of gas transfer aided by tracer experiments is calculated as:

$$K_{600wind} = 0.45\mu^{1.6}(Sc/600) - \alpha \quad (3.6)$$

Where, μ being the wind speed (m s^{-1}), α is the flexible power function influenced by wind speed ($\alpha = 0.6667$ when $\mu < 3.6 \text{ ms}^{-1}$, and $\alpha = 0.5$ when $\mu > 3.6 \text{ ms}^{-1}$). Sc being the Schmidt number suggested at a particular water temperature for Radon. To normalize gas transfer velocity to Schmidt number for freshwater CO_2 at 20°C , Sc is divided by 600 to normalize the gas transfer velocity, which is defined as the ratio of kinematic viscosity (ν) to the molecular diffusion coefficient (D_m) calculated as:

$$Sc = \nu / D_m \quad (3.7)$$

The molecular diffusivity coefficient being the function of temperature (T), is explained as:

$$D_m = 10^{-(1.59+980/(T+273))} \quad (3.8)$$

The kinematic viscosity (ν) is the ratio of the absolute viscosity (μ) to the density (ρ) of the water at a measured temperature:

$$\nu = \mu / \rho \quad (3.9)$$

By adopting Eq. 3.9, the diffusive flux of Radon at the air-water interface is calculated. F_{atm} is found to be influenced by gas transfer velocity (k), partition coefficient (α), and varying

Radon in the air (C_{air}) and water interface (C_w). The average loss of Radon to the atmosphere at the air-water interface is $28.06 \text{ Bq m}^{-2} \text{ h}^{-1}$.

4.2.2. Sediment diffusive radon fluxes

The ^{222}Rn flux will also diffuse from aquifer sediments to the water when the sediments essentially contain radon source elements. The sediment diffused radon flux is calculated, attempting equation suggested by [39] as noted below.

$$F_{sed} = (\lambda n D_m)^{0.5} (C_{eq} - C_o) \quad (3.10)$$

Here, F_{sed} suggests the sediment diffused radon fluxes represented in $\text{Bq m}^{-2} \text{ h}^{-1}$, λ portrays the radon decay constant as 0.181 d^{-1} , n represents the sediment porosity, C_o and C_{eq} propose Radon in sediments and water column expressed in Bq m^{-3} . The grain size study attempted for the study area sediments ranges between 0.37 to 0.46 and ^{222}Rn in water samples ranges between 127.39 and 2643.41 Bq m^{-3} . D_m represents the molecular diffusion coefficient for salinity 34.0 at 18°C found to range between 1.75×10^{-5} and $1.98 \times 10^{-5} \text{ cm}^2 \text{ s}^{-1}$ (Jahne et al. 1987) [40]. By simplifying equation (3.10), the variation in net radon fluxes across the sediment-water interface was found between -0.14 to $1.48 \text{ Bq m}^{-2} \text{ h}^{-1}$. More significant radon fluxes across the sediment-water interface might be due to the porous and permeable sand formation isolated in the study area found negligible compared with the total radon fluxes.

4.2.3. Inventory of excess radon and radium fluxes

Burnett and Dulaiova 2003 [41] have proposed the impact of tides on radon variability to assess the excess Radon, which is defined as the artifact of excess ^{222}Rn ($^{222}\text{Rn} - ^{226}\text{Ra}$) in water and water depth (h) calculated adopting equation suggested below:

$$\text{Excess } ^{222}\text{Rn} (\text{Bq m}^{-3}) = \text{Total } ^{222}\text{Rn} (\text{Bq m}^{-3}) - ^{226}\text{Ra} (\text{Bq m}^{-3}) \quad (3.11)$$

The excess ^{222}Rn in water has been calculated considering ^{226}Ra concentrations estimated by [11] in Sankarabarani estuary (0.629 Bq m^{-3}) were considered for the present study due to proximity, similar geological and tidal conditions. The ^{226}Ra concentration was deducted from the total ^{222}Rn to precise Radon supported from radium-226. The radon flux (RF) variations of the study area ranged between 9.5 to $36.2 \text{ Bq m}^{-2} \text{ h}^{-1}$.

4.2.4. Tidal influence

The radon fluxes seem to be influenced by tidal fluctuations. During low tide (F_{out}) radon is found to be released from aquifer to sea, and during high tide (F_{in}), Radon is found to be supplemented from sea to groundwater.

4.2.5. Estimation of mixing loss and net radon flux

Radon mixing loss is mainly due to the radon movement out of the system due to mixing activities at nearshore when higher radon groundwater mixes with lower radon seawater [37, 42, 35].

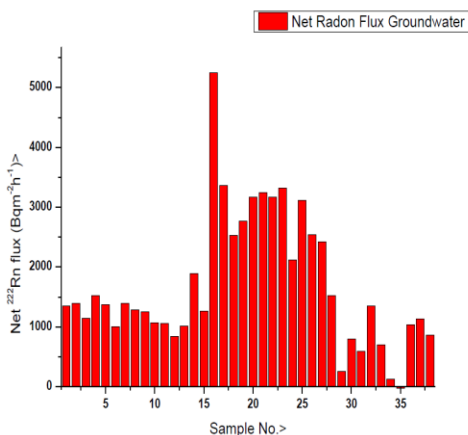


Figure 4. Groundwater radon fluxes

After stabilizing Radon concerning tidal variations, loss to the atmosphere, and diffusion from sediment, the net radon flux isolated should equilibrate SGD attributed Radon and those lost to the ocean as mixing loss. [35] have suggested mixing loss from the negative values of radon fluxes. More significant mixing loss signifies a larger SGD supply and is about 20% from the total radon fluxes [35]. The groundwater net mixing loss was found to range between -25.41 to 5248.94 Bq m⁻² h⁻¹ (Figure 4). Negative values in the mixing loss calculation suggest the absence of SGD fluxes and negative values observed in the groundwater samples suggest the influence of recirculated seawater to contribute about 90% of the total SGD happening globally [43].

4.2.6. Net fluxes of Radon

SGD fluxes were attempted by dividing the overall radon fluxes with those observed in groundwater samples. For the present study, groundwater end members were considered due to the greater availability of Radon in groundwater samples, indicating greater mobility.

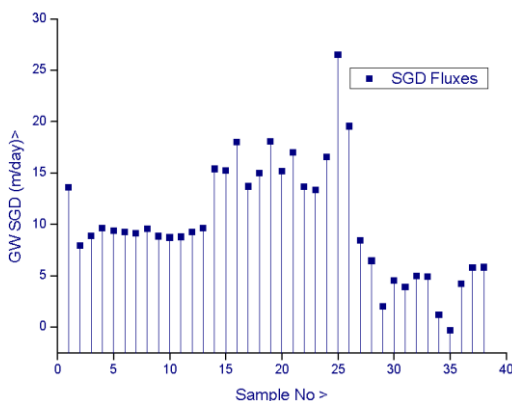


Figure 5. Groundwater attributed SGD fluxes

The calculated SGD fluxes for groundwater samples range between -1.0 to 26.5 with an average of 10.32 m day⁻¹. More significant fluxes observed in specific locations confined to the southern part of Cuddalore and Nagapattinam districts suggest that the influence of fresh groundwater discharge and lower observed in north Cuddalore and Vedaranyam localities suggests the influence of recirculated seawater altering the chemical composition of groundwater along with radon availability (Figure. 5).

4.3. Spatial representation of data sets

An attempt has been made to correlate Radon, salinity spatially, and temperature for groundwater samples collected (Fig. 6). Lower Radon, lower salinity, and temperature were recorded along with the northern parts of the study area, demarcating the lower significance of fresh, terrestrial SGD. In the central parts of the study area, higher Radon, lower and intermediate salinity, and greater temperatures confirmed the fresh SGD and southern parts of the study domain recorded with lower to intermediate Radon, intermediate to higher salinity, and intermediate to higher temperature signifying chances of recirculated SGD. In general, northern parts of the study area are found to be influenced by seawater intrusion, central parts of the study area are noted with fresh, terrestrial SGD discharge, and the southern part of the study area is found to be influenced by recirculated SGD. The above observations confirmed with TIR images showing zones of discharge confined to central parts of the study area.

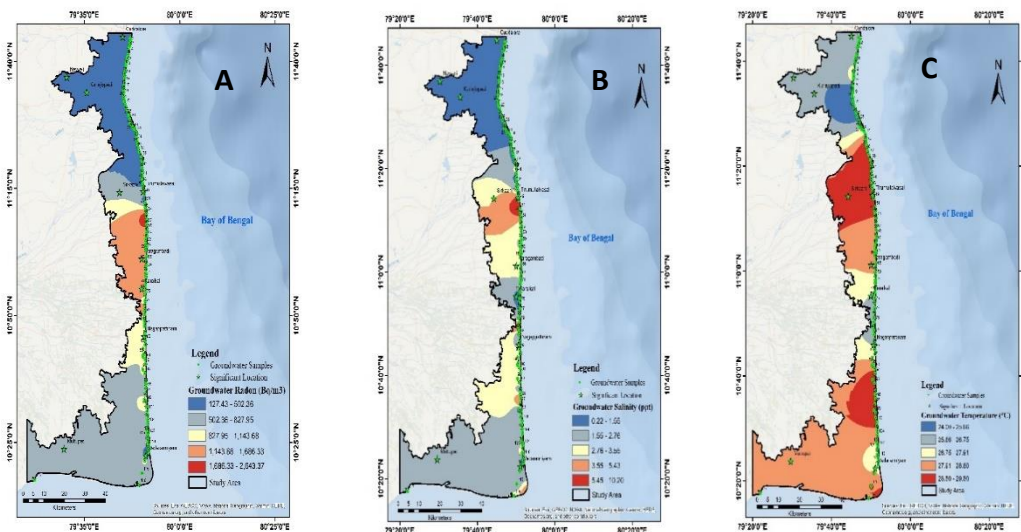


Figure 6. Spatial plots for (A) Radon, (B) Salinity, and (C) Temperature

5. Conclusion

The East Coast of Tamil Nadu has been influenced by recent human development that has threatened groundwater quality in the coastal aquifers. An attempt has been made to

find the submarine groundwater discharge (SGD) zone by processing LANDSAT 8 data, and flux has been calculated using the radon mass balance model. Thermal anomalies given freshwater flow were found to range between 24° C to 28° C prominent along with the central parts of the study area signifying sources of terrestrial SGD and lower anomalies noted in northern and southern parts of the study are suggest the influence of seawater intrusion and recirculated seawater. Radon attributed SGD flux attempted adopting radon mass balance model suggest more significant fluxes 26.5 m day⁻¹ and found to be influenced by groundwater velocity and hydraulic gradient. More significant fluxes were noted in a nutshell in central parts of the study area, indicating terrestrial groundwater discharge and lower fluxes confined to northern and southern parts of the study domain suggest the influence of seawater intrusion and recirculated seawater. Spatial plot attempted for Radon, salinity, and temperature also confirm the possibility of three significant discharge types, which was also in analogy with SST calculated for the present study area.

References

- [1] W. C. Burnett, H. Dulaiova, Radon as a tracer of submarine groundwater discharge into a boat basin in Donmalucata, Sicily, *Continental Shelf Research*, 26 (2006) 862-873. [\[DOI\]](#)
- [2] W. S. Moore, J. L. Sarmiento, R. M. Key, Submarine groundwater discharge revealed by 228 Ra distribution in the upper Atlantic Ocean, *Nature Geoscience*, 1 (2008) 309-311.
- [3] J.M. Bishop, C.R Glenn, D.W. Amato, H. Dulai, Effect of land use and groundwater flow path on submarine groundwater discharge nutrient flux, *Journal of Hydrology: Regional Studies*, 11(2017) 194-218. [\[DOI\]](#)
- [4] C. P. Slomp, P. Van Cappellen, Nutrient inputs to the coastal ocean through submarine groundwater discharge: controls and potential impact, *Journal of Hydrology*, 295 (2004) 64-86. [\[DOI\]](#)
- [5] G. Kim, P.W. Swarzenski, (2010) Submarine groundwater discharge (SGD) and associated nutrient fluxes to the coastal ocean, In *Carbon and nutrient fluxes in continental margins*, Springer, 529-538. [\[DOI\]](#)
- [6] W.S. Moore, The effect of submarine groundwater discharge on the ocean, *Annual review of marine science*, 2 (2010) 59-88. [\[DOI\]](#)
- [7] N. N. Rabalais, T.R. E.urner, C.D. Justi, Q. Dortch, W.J. Wiseman, B.K.S. Gupta, Nutrient changes in the Mississippi River and system responses on the adjacent continental shelf, *Estuaries*, 19 (1996) 386-407.

- [8] S.P. Seitzinger, E. Mayorga, A. F. Bouwman, C. Kroeze, A. H. W. Beusen, G. Billen, G. Van Drecht, E. Dumont, B. M. Fekete, J. Garnier, J. A. Harrison, Global River nutrient export: A scenario analysis of past and future trends, *Global Biogeochemical Cycles*, 24 (2010) 1-16. [\[DOI\]](#)
- [9] R. Prakash, K. Srinivasamoorthy, S.M. Sundarapandian, C. Nanthakumar, S. Gopinath, K. Saravanan, F. Vinnarasi, Submarine groundwater discharge from an urban estuary to southeastern Bay of Bengal, India: revealed by trace element fluxes, *Archives of Environmental Contamination and Toxicology*, 80 (2021) 208-233.
- [10] R. Prakash, K. Srinivasamoorthy, S. Gopinath, K. Saravanan, F. Vinnarasi., Approximation of submarine groundwater discharge and allied nutrient fluxes to the Bay of Bengal, India using nutrient mass balance, *Environmental Earth Sciences*, 80 (2021) 1-22.
- [11] G. Saravanan, G. Ponnnumani, K. Srinivasamoorthy, R. Prakash, S. Gopinath, C. Babu, F. Vinnarasi, D. Karunanidhi, T. Subramani, (Estimating groundwater inputs from Sankarabarani River Basin, South India to the Bay of Bengal evaluated by Radium (226Ra) and nutrient fluxes, *International Journal of Civil, Environmental and Agricultural Engineering*, 2 (2020) 17-32. [\[DOI\]](#)
- [12] R. Prakash, K. Srinivasamoorthy, S. Gopinath, K. Saravanan, Submarine groundwater discharge as sources for dissolved nutrient fluxes in Coleroon river estuary, Bay of Bengal, India, *Journal of Contaminant Hydrology*, 233 (2020) 103660. [\[DOI\]](#)
- [13] J. L. Bowen, K. D. Kroeger, G. Tomasky, W.J. Pabich, M. L. Cole, R. H. Carmichael, I. Valiela, A review of land-sea coupling by groundwater discharge of nitrogen to New England estuaries: mechanisms and effects, *Applied geochemistry*, 22 (2007) 175-191. [\[DOI\]](#)
- [14] W. S. Moore, Large groundwater inputs to coastal waters revealed by 226Ra enrichments, *Nature*, 380 (1996) 612-614.
- [15] M. Schubert, J. Scholten, A. Schmidt, J. F. Comanducci, M. K. Pham, U. Mallast, K. Knoeller, Submarine groundwater discharge at a single spot location: evaluation of different detection approaches, *Water*, 6 (2014) 584-601. [\[DOI\]](#)
- [16] J. L. Kelly, C.R. Glenn, P.G. Lucey, High-resolution aerial infrared mapping of groundwater discharge to the coastal ocean, *Limnology and Oceanography: Methods*, 11 (2013) 262-277. [\[DOI\]](#)
- [17] W.S. Banks, R.L. Paylor, W.B. Hughes, Using Thermal-Infrared Imagery to Delineate Ground-Water Discharged, *Groundwater*, 34 (1996) 434-443. [\[DOI\]](#)
- [18] M.P. Anderson, Heat as a groundwater tracer, *Groundwater*, 43 (2005) 951-968. [\[DOI\]](#)

- [19] J. Wilson, C. Rocha, Regional scale assessment of Submarine Groundwater Discharge in Ireland combining medium resolution satellite imagery and geochemical tracing techniques, *Remote Sensing of Environment*, 119 (2012) 21-34. [\[DOI\]](#)
- [20] E. J. Pluhowski, (1972). Hydrologic interpretations based on infrared imagery of Long Island, New York, US Government Printing Office, 1-25.
- [21] W.C. Burnett, P.K. Aggarwal, A. Aureli, H. Bokuniewicz, J.E. Cablee, M.A. Charette, E. Kontarg, S. Krupa, K.M. Kulkarni, A. Loveless, W.S. Moore, J.A. Oberdorfer, J. Oliveiral, N. Ozyurt, P. Povinec, A.M.G. Privitera, R. Rajar, R.T. Ramessur, J.V. Turneru, Quantifying submarine groundwater discharge in the coastal zone via multiple methods, *Science of the total Environment*, 367 (2006) 498-543. [\[DOI\]](#)
- [22] D. Corbett, W. Burnett, P. Cable, S. Clark, A multiple approach to the determination of radon fluxes from sediments, *Journal of Radioanalytical and Nuclear Chemistry*, 236 (1998) 247-253. [\[DOI\]](#)
- [23] A. Rajesh Kanna, K. Srinivasamoorthy, G. Ponnurmani, S. Gopinath, R. Prakash, D. Karunanidhi, F. Vinnarasai, Assessment of Radon in groundwater and associated human risk from Sankarabarani River Sub Basin, Southern India.
- [24] Central groundwater board, District Groundwater Brochure (2008) Nagapattinam District Tamil Nadu.
- [25] Central groundwater board, District Groundwater Brochure (2009) Cuddalore District Tamil Nadu.
- [26] Central groundwater board, Pilot Project Report on Aquifer mapping in Lower Vellar watershed (December-2015), Cuddalore district, Tamilnadu. I: 10.26524/ijceae1912
- [27] M. Raghavayya, M.A.R. Iyengar, P. M. Markose, Estimation of radium-226 by emanometry, *Bulletin of Radiation Protection*, 3(1980)
- [28] M. Blackett, Early analysis of Landsat-8 thermal infrared sensor imagery of volcanic activity, *Remote sensing*, 6 (2014) 2282-2295. [\[DOI\]](#)
- [29] D. Jeevalakshmi, S. Narayana Reddy, B. Manikiam, Land surface temperature retrieval from LANDSAT data using emissivity estimation, *International Journal of Applied Engineering Research*, 12 (2017) 9679-9687.
- [30] C.W. Fairall, E.F. Bradley, J.S. Godfrey, G.A Wick, J.B. Edson, G. S. Young, Cool-skin and warm-layer effects on sea surface temperature, *Journal of Geophysical Research: Oceans*, 101 (1996) 1295-1308. [\[DOI\]](#)

- [31] C.J. Donlon, M. Martin, J. Stark, J. Roberts-Jones, E. Fiedler, W. Wimmer, The operational sea surface temperature and sea ice analysis (OSTIA) system, *Remote Sensing of Environment*, 116 (2012) 140-158. [\[DOI\]](#)
- [32] A. Schmidt, C.E. Stringer, U. Haferkorn, M. Schubert, Quantification of groundwater discharge into lakes using radon-222 as naturally occurring tracer, *Environmental Geology*, 56 (2009) 855-863.
- [33] R. K. Dale, D. C. Miller, Spatial and temporal patterns of salinity and temperature at an intertidal groundwater seep, *Estuarine, Coastal and Shelf Science*, 72 (2007) 283-298. [\[DOI\]](#)
- [34] M. Schubert, A. Paschke, D. Bednorz, W. Bürkin, T. Stieglitz, Kinetics of the water/air phase transition of Radon and its implication on detection of radon-in-water concentrations: practical assessment of different on-site radon extraction methods, *Environmental science & technology*, 46 (2012) 8945-8951. [\[DOI\]](#)
- [35] K. Srinivasamoorthy, G. Ponnunani, R. Prakash, S. Gopinath, K. Saravanan, F. Vinnarasi, Tracing groundwater inputs to Bay of Bengal from Sankarabaran River Basin, Pondicherry, India, using continuous radon monitoring, *International Journal of Environmental Science and Technology*, 16 (2019) 5513-5524.
- [36] W.C. Burnett, H. Bokuniewicz, M. Huettel, W.S. Moore, M. Taniguchi, Groundwater and pore water inputs to the coastal zone, *Biogeochemistry*, 66 (2003) 3-33.
- [37] Y. Zhang, H. Li, X. Wang, C. Zheng, C. Wang, K. Xiao, L. Wan, X. Wang, X. Jiang, H. Guoab, Estimation of submarine groundwater discharge and associated nutrient fluxes in eastern Laizhou Bay, China using ²²²Rn, *Journal of Hydrology*, 533 (2016) 103-113. [\[DOI\]](#)
- [38] K. Eckerman, J. Harrison, H.G. Menzel, C.H. Clement, ICRP publication 119: compendium of dose coefficients based on ICRP publication 60, *Annals of the ICRP*, 41 (2012) 1-130. [\[DOI\]](#)
- [39] C.S. Martens, G.W. Kipphut, J.V. Klump, Sediment-water chemical exchange in the coastal zone traced by in situ radon-222 flux measurements, *Science*, 208 (1980) 285-288. [\[DOI\]](#)
- [40] B. Jahne, K.O. Munnich, R. Bosinger, A. Dutzi, W. Huber, P. Libner, On the parameters influencing air-water gas exchange, *Journal of Geophysical Research: Oceans*, 92 (1987) 1937-1949. [\[DOI\]](#)
- [41] W.C. Burnett, H. Dulaiova, Estimating the dynamics of groundwater input into the coastal zone via continuous radon-222 measurements, *Journal of environmental radioactivity*, 69 (2003) 21-35. [\[DOI\]](#)

- [42] R. Prakash, K. Srinivasamoorthy, S. Gopinath, K. Saravanan, F. Vinnarasi, G. Ponnunmani, P. Anandhan, Radon isotope assessment of submarine groundwater discharge (SGD) in Coleroon River Estuary, Tamil Nadu, India, *Journal of Radioanalytical and Nuclear Chemistry*, 317 (2018) 25-36.
- [43] I. Kim, G. Kim, Large fluxes of rare earth elements through submarine groundwater discharge (SGD) from a volcanic island, Jeju, Korea, *Marine Chemistry*, 127 (2011) 12-19. [\[DOI\]](#)
- [44] W.C. Burnett, M. Taniguchi, J. Oberdorfer, Measurement and significance of the direct discharge of groundwater into the coastal zone, *Journal of Sea Research*, 46 (2001) 109-116. [\[DOI\]](#)

Acknowledgment

This research was funded by NESSO- National Centre for Earth Science Studies, Ministry of Earth Sciences, Govt. of India through Unravelling Submarine Groundwater Discharge (SGD) zones along the Indian Subcontinent and its Islands (Mission SGD)- Pilot Study, Submarine Groundwater Discharge (SGD), (NCESS/MOES/ 402/GAI/2019 & 29-03-2019). The Radon analysis was performed using the equipment procured from a project supported by the Department of Science Technology and Engineering Research Board (Grant No. EMR/2015/001101).

Acknowledgements:

Conflict of interest: NIL

About The License: © 2021 The Authors. This work is licensed under a Creative Commons Attribution 4.0 International License which permits unrestricted use, provided the original author and source are credited.